ATP Binding Enables Broad Antibiotic Selectivity of Aminoglycoside Phosphotransferase(3′)-IIIa – An Elastic Network Analysis

Silke A. Wieninger[1], Engin H. Serpersu[2] and G. Matthias Ullmann[1,*]

[1] Computational Biochemistry / Bioinformatics, University of Bayreuth, Universitätsstr. 30, BGI, 95447 Bayreuth, Germany

[2] Department of Biochemistry and Cellular and Molecular Biology, The University of Tennessee, Knoxville, Tennessee, 37996, USA

[*] Corresponding Author

Email: Matthias.Ullmann@uni-bayreuth.de

Telephone: +49-921-55-3545

Fax: +49-921-55-3071

Supplemental Data

Derivation of eq 10

For a diagonalisable $n \times n$ square matrix A, denote the pseudo-inverse by $\tilde{A}^{-1}$. If A is invertible, then of course $\tilde{A}^{-1} = A^{-1}$. Denote the unit vectors by e_i and the vector with all entries 1 by e.

Let $\lambda_1 \leq ... \leq \lambda_n$ be the eigenvalues of A, $\Lambda = \mathrm{diag}(\lambda_1, ..., \lambda_n)$, and U the orthogonal matrix with rows given by the normalized eigenvectors of A. Then

$$A = U^{\mathrm{T}} \Lambda U \quad \text{and} \quad \tilde{A}^{-1} = U^{\mathrm{T}} \tilde{\Lambda}^{-1} U \tag{1}$$

Further let $v = (v_1, ..., v_n)^{\mathrm{T}} = Ue_i$, and note that v is a unit vector, $\sum_k v_k^2 = 1$. Then

$$A_{ii} = e_i \cdot Ae_i = Ue_i \cdot \Lambda U e_i = v \cdot \Lambda v = \sum_{k=1}^{n} \lambda_k v_k^2. \tag{2}$$

If A is invertible,

$$A_{ii}^{-1} = Ue_i \cdot \Lambda^{-1} U e_i = \sum_{k=1}^{n} v_k^2 \frac{1}{\lambda_k} = \frac{1}{A_{ii}} \sum_{k,l=1}^{n} v_k^2 v_l^2 \frac{\lambda_l}{\lambda_k} \tag{3}$$

Now we use the fact that $\frac{a}{b} + \frac{b}{a} \geq 2$ for any strictly positive reals a, b, and obtain

$$\begin{aligned} \sum_{k,l=1}^{n} v_k^2 v_l^2 \frac{\lambda_l}{\lambda_k} &= \sum_{k<l} v_k^2 v_l^2 \left(\frac{\lambda_l}{\lambda_k} + \frac{\lambda_k}{\lambda_l} \right) + \sum_k v_k^4 \geq 2 \sum_{k<l} v_k^2 v_l^2 + \sum_k v_k^4 \\ &= \sum_{k,l} v_k^2 v_l^2 = \sum_k v_k^2 \sum_l v_l^2 = 1. \end{aligned} \tag{4}$$

Therefore, if A is invertible, it follows that

$$\tilde{A}_{ii}^{-1} \geq \frac{1}{A_{ii}}. \tag{5}$$

The Kirchhoff matrix is a symmetric, positive semi-definite matrix. The eigenvalue 0 has multiplicity 1 and corresponding eigenvector e. We obtain in the same way as in Equations 3 and 4

$$\tilde{A}_{ii}^{-1} = \frac{1}{A_{ii}} \sum_{k,l=2}^{n} v_k^2 v_l^2 \frac{\lambda_l}{\lambda_k} \geq \frac{1}{A_{ii}} \sum_{k=2}^{n} v_k^2 \sum_{l=2}^{n} v_l^2 = \frac{1}{A_{ii}} (1 - v_1^2)^2. \tag{6}$$

As e is an eigenvector for λ_1,

$$v_1^2 = \frac{(e_i \cdot e)^2}{|e|^2} = \frac{1}{n}, \tag{7}$$

and it follows

$$\tilde{A}_{ii}^{-1} \geq \frac{1}{A_{ii}} \left(\frac{n-1}{n} \right)^2. \tag{8}$$

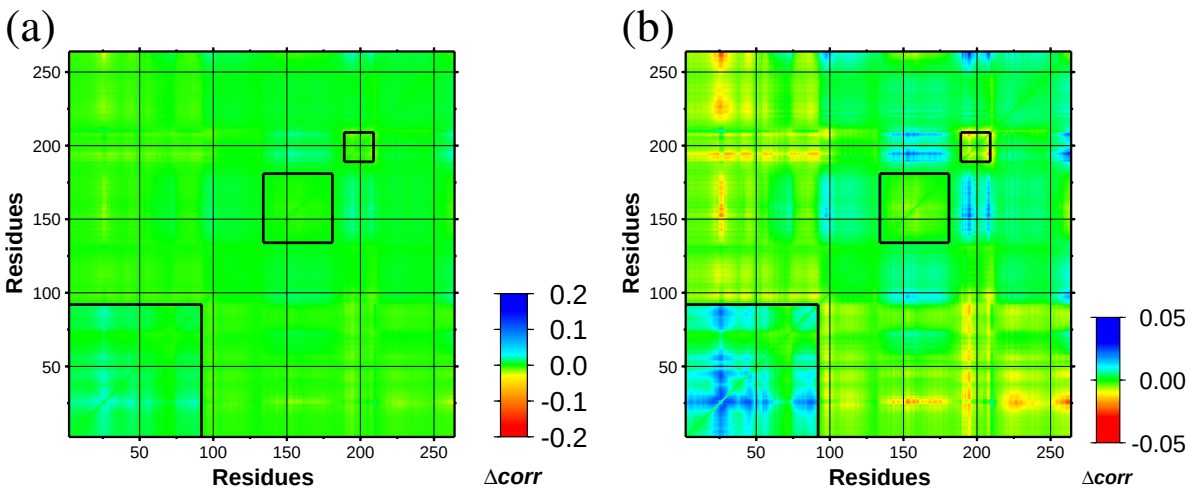

Figure S 1: Difference correlation plot showing the deviation from additivity of the effects of substrate binding. The correlation differences of X[APH-Nuc-Kana] minus M_{kan}[APH] are subtracted from the sum of the single effects, *i.e.* the difference correlations of X[APH-Nuc-Kana] minus M_{kan}[APH-Kana] added to the difference correlations of X[APH-Nuc-Kana] minus M_{kan}[APH-Nuc]. The highest absolute value of deviation is < 0.05. (a) Color scale corresponds to color scale of Figure 2b,c,d. (b) Using a color scale ranging from -0.05 to $+0.05$ shows that small deviations from additivity occur in the regions affected by substrate, especially nucleotide-binding.

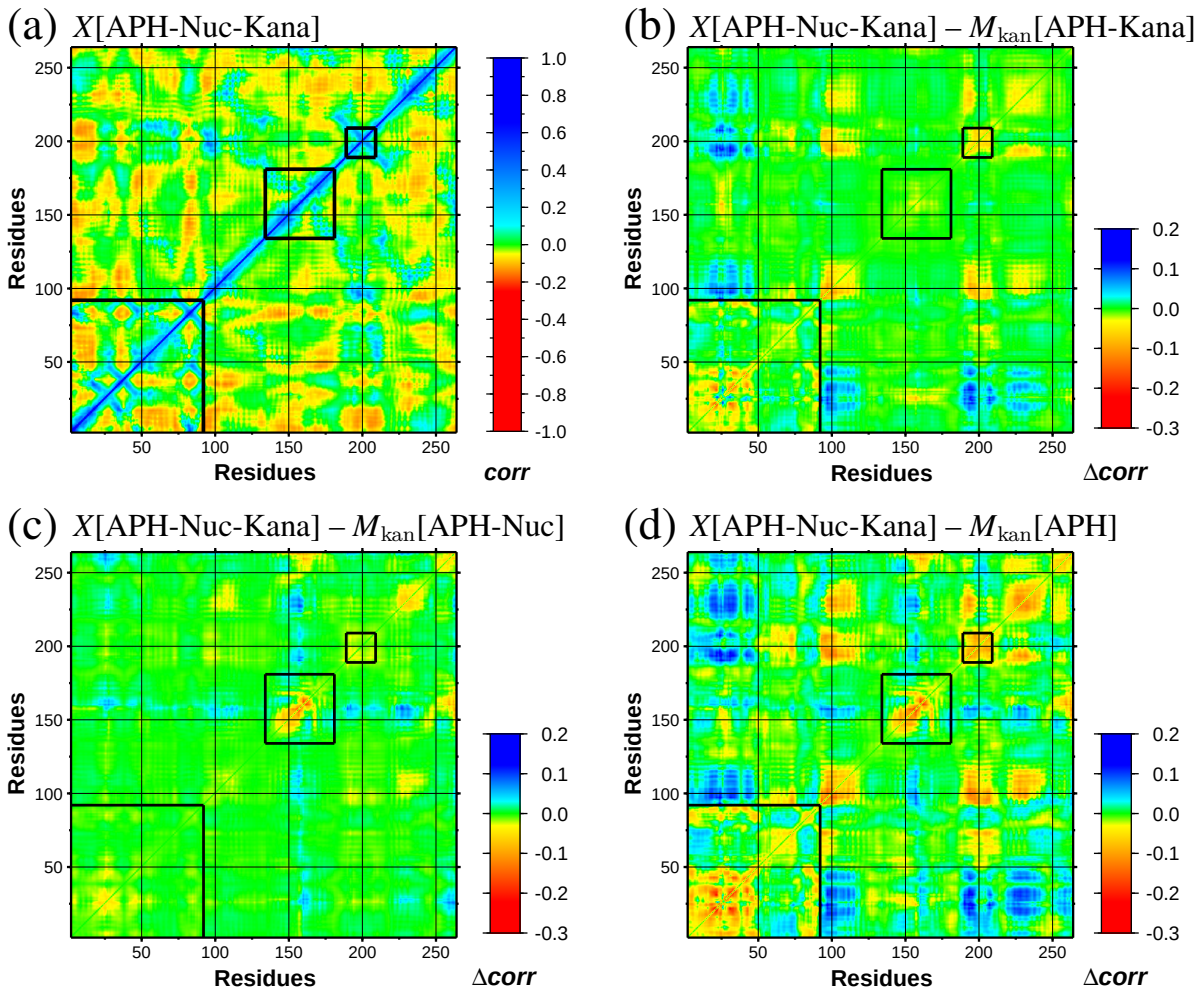

Figure S 2: Correlated motions of APH calculated with the ANM for X[APH-Nuc-Kana], using a cutoff radius of 10Å. While the classification into three protein domains is less obvious than from GNM calculations, the substrate-dependent correlation differences are very similar to the differences obtained with the GNM. (a) Correlation plot of X[APH-Nuc-Kana]. (b) The difference correlation plot of original X[APH-Nuc-Kana] complex minus correlations of model complex M_{kan}[APH-Kana] shows the effect of nucleotide binding to the binary APH-kanamycin complex. (c) The difference correlation plot of original X[APH-Nuc-Kana] complex minus correlations of model complex M_{kan}[APH-Nuc] shows the effect of kanamycin binding to the binary APH-nucleotide complex. (d) The difference correlation plot of original X[APH-Nuc-Kana] complex minus correlations of model complex M_{kan}[APH] shows that the effects of binding of both substrates are nearly additive.

Table S 1: Classification of nodes in dynamic domains calculated for the different APH structures.

	Domain I	Domain II	Domain III
X[APH]	5-91	92-129, 180-249	130-179, 250-264
M_{nuc}[APH]	2-95, 197-202	96-136, 180-249	137-179, 250-264
M_{kan}[APH]	2-95	96-136, 180-255	137-179, 256-264
M_{neo}[APH]	2-95	96-136, 180-255	137-179, 253-264

Table S 2: Comparison between experimental and theoretical B-factors for different structures and cutoff distances d_{cut}. The linear correlation coefficient ρ between experimental B-factors (x_i) and calculated B-factors (y_i) is given by $\rho = \frac{\sum(x_i-x)(y_i-y)}{\sqrt{\sum(x_i-x)^2\sum(y_i-y)^2}}$. x and y are the mean values of the corresponding B-factors.

	1J7I	1J7U	1L8T	2B0Q
Substrate(s)	–	MgAMPPNP	MgADP, kanamycin A	MgADP, neomycin B
ρ ($d_{\mathrm{cut}} = 6$ Å)	0.14	0.32	0.15	0.38
ρ ($d_{\mathrm{cut}} = 7$ Å)	0.26	0.54	0.48	0.47
ρ ($d_{\mathrm{cut}} = 8$ Å)	0.25	0.55	0.55	0.50
ρ ($d_{\mathrm{cut}} = 9$ Å)	0.29	0.51	0.57	0.49

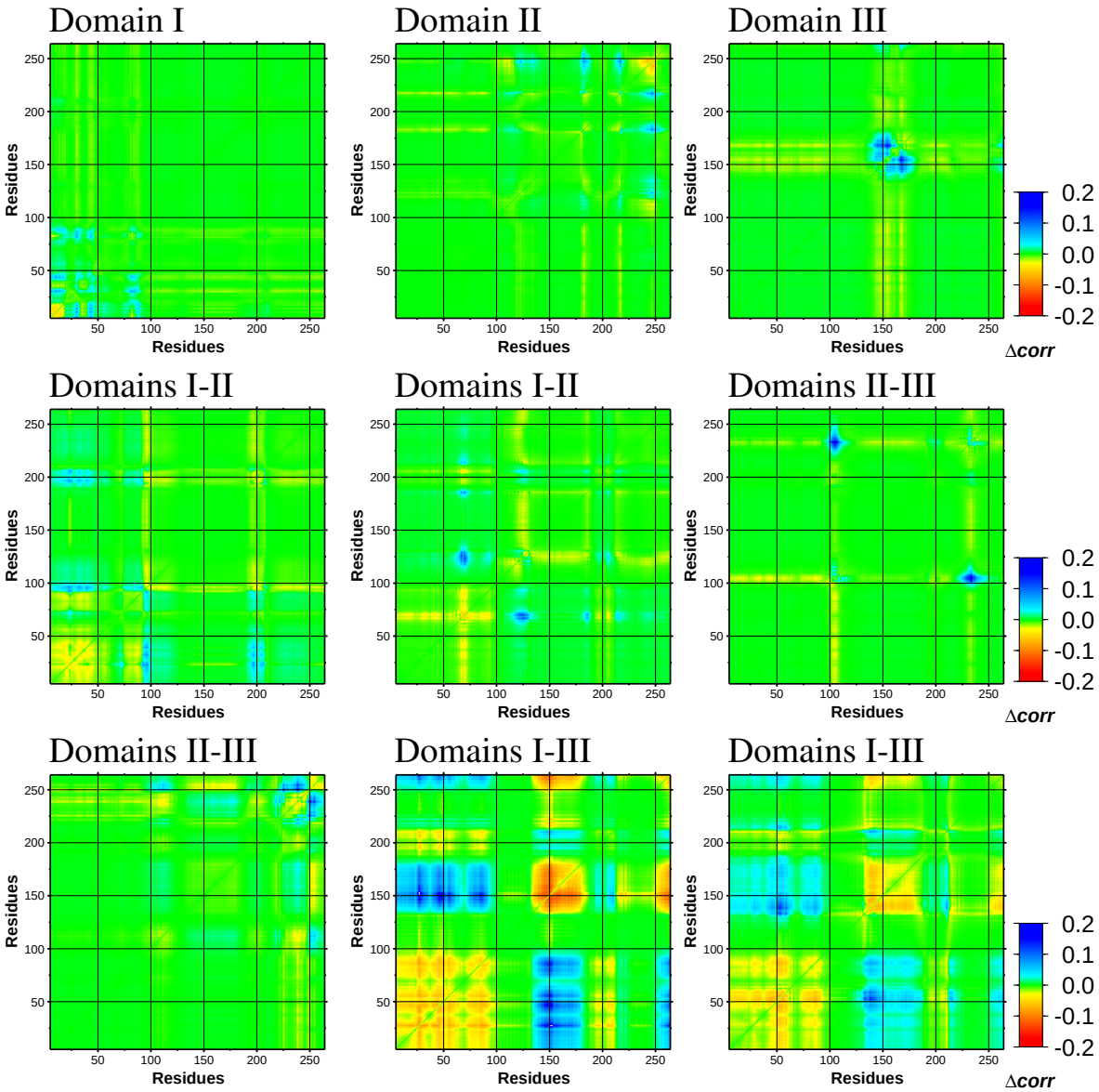

Figure S 3: Correlation change upon binding of a pseudo-substrate to *X*[APH]. The correlations of the structure with pseudo-substrate are subtracted from the correlations of *X*[APH]. The pseudo-substrates are either bound on the surface of one domain (first row), or at the interface between two domains (second and third row). Most pseudo-substrates have only minor and very localized effects on the correlations. Only the two pseudo-substrates lying between domain I and III have a large effect on the correlations, which is comparable to the effect of real ligand binding.

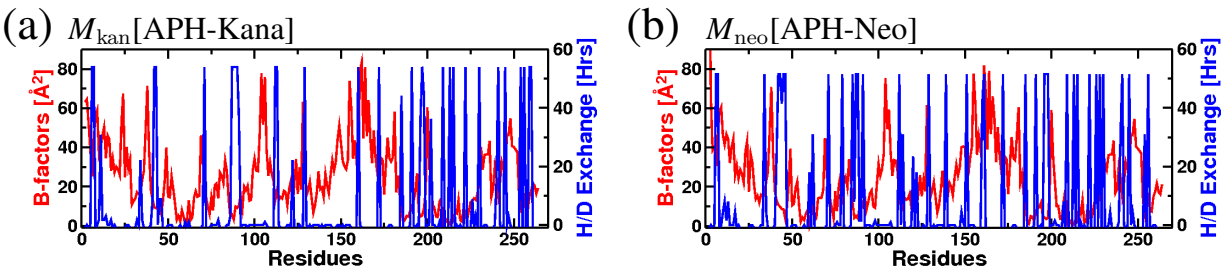

Figure S 4: NMR H/D exchange times (blue curve) and theoretical B-factors (red curve) for the antibiotic complexes of APH. (a) M_{kan}[APH-Kana] and (b) M_{neo}[APH-Neo] are used for the calculations. The theoretical B-factors are shifted such that the lowest B-factor of each structure is zero. Peaks never exchanged in 96 hours are cut off at 54.0 hr line and 51.5 hr line. A time value of zero means that the hydrogen exchange occurred faster than the start of the acquisition of the first spectrum (3-4 min of delay to start data acquisition). Exchange times are only measured for about half of the residues. Generally, long H/D exchange times correspond to low B-factors, and vice versa.

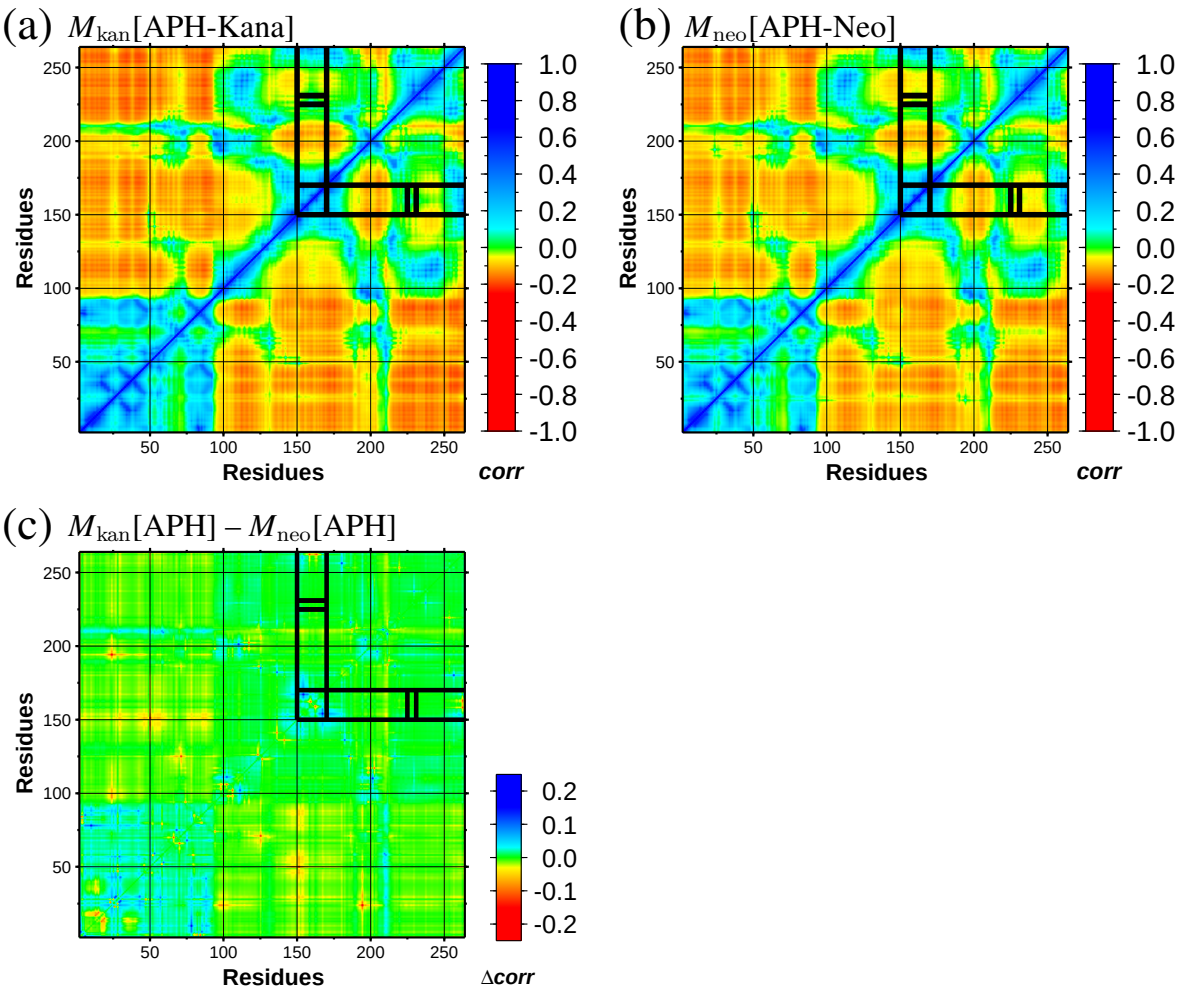

Figure S 5: Correlated motion of APH in binary complexes with kanamcyin and neomycin. (a) Correlation plot of M_{kan}[APH-Kana]. (b) Correlation plot of M_{neo}[APH-Neo]. The positive correlations of residues 157 to 162 of domain III to each other and to the C-terminal residues is higher in the neomycin-bound form. The correlations between residues 157 to 162 of domain III and residues 226 to 230 of domain II are approx. zero in M_{kan}[APH-Kana], because they are strongly connected over kanamycin. With neomycin, the two stretches are anticorrelated. (c) Correlation differences between M_{kan}[APH] and M_{neo}[APH] arising from structural differences between X[APH-Nuc-Kana] and X[APH-Nuc-Neo]. The correlation differences of residues 157 to 162 in plots a and b do not arise from structural differences, but are due to binding of the antibiotic.